Available online at www.sciencedirect.com
SCIENCE DIRECT
Biochimica et Biophysica Acta 1717 (2005) 109 – 117
BIOCHIMICA ET BIOPHYSICA ACTA
BBA
http://www.elsevier.com/locate/bba

Sodium-dependent glucose transporter reduces peroxynitrite and cell injury caused by cisplatin in renal tubular epithelial cells

Akira Ikari [a,b,*], Yoshiaki Nagatani [a], Mitsutoshi Tsukimoto [a], Hitoshi Harada [a], Masao Miwa [b], Kuniaki Takagi [a]

[a] *Department of Environmental Biochemistry and Toxicology, School of Pharmaceutical Sciences, University of Shizuoka, 52-1 Yada, Shizuoka 422-8526, Japan*
[b] *Department of Pharmaco-Biochemistry, School of Pharmaceutical Sciences, University of Shizuoka, 52-1 Yada, Shizuoka 422-8526, Japan*

Received 6 July 2005; received in revised form 27 September 2005; accepted 6 October 2005
Available online 25 October 2005

Abstract

Cisplatin causes nephropathy accompanied by two types of cell death, necrosis and apoptosis, according to its dosage. The mechanisms of necrosis are still unclear. In this study, we examined how high doses of cisplatin induce cell injury and whether a high affinity sodium-dependent glucose transporter (SGLT1) has a cytoprotective function in renal epithelial LLC-PK_1 cells. Cisplatin decreased in transepithelial electrical resistance (TER) and increased in the number of necrotic dead cells in a time dependent manner. Phloridzin, a potent SGLT1 inhibitor, enhanced both TER decrease and increase of necrotic dead cells caused by cisplatin. Cisplatin increased in the intracellular nitric oxide, superoxide anion and peroxynitrite productions. Phloridzin enhanced the peroxynitrite production caused by cisplatin. The intracellular diffusion of ZO-1 and TER decrease caused by cisplatin were inhibited by *N*-nitro-L-arginine methyl ester, a nitric oxide synthase inhibitor. Protein kinase C was not involved in the cisplatin-induced injury. 5,10,15,20-tetrakis-(4-sulfonatophenyl)-porphyrinato iron (III) and reduced glutathione, peroxynitrite scavengers, inhibited the cisplatin-induced ZO-1 diffusion, TER decrease, and increase of necrotic dead cells. These results suggest that peroxynitrite is a key mediator in the nephrotoxicity caused by high doses of cisplatin. SGLT1 endogenously carries out the cytoprotective function by the reduction of peroxynitrite production.

Keywords: Cisplatin; Cytoprotection; Peroxynitrite; Sodium-dependent glucose transporter; Tight junction; ZO-1

1. Introduction

Cisplatin and its analogs of platinum complexes are effective chemotherapeutic agents against a variety of solid tumors of the ovary, testis, bladder, head and neck, cervix, and lung. However, its use is often limited due to its adverse effects such as nephrotoxicity, leading to acute renal failure and the long-term impairment of renal function [1,2]. The nephrotoxic effect of cisplatin is characterized by definitive histological changes and is primarily found in the S3 segment of the proximal tubule [3,4]. Cisplatin nephrotoxicity is associated with increases in reactive oxygen species (ROS) and reactive nitrogen species (RNS) such as superoxide anion, hydroxyl radical, and peroxynitrite [5,6]. In cisplatin chemotherapy, it is clinically important to arrest the development of nephrotoxicity, but effective therapeutic or prophylactic agents have not yet been found.

Studies on animals have established that tubular injury plays a central role in the reduction of the glomerular filtration rate in acute tubular necrosis. A number of studies have shown that cisplatin induces apoptosis or necrosis in renal tubular epithelial cells in vivo and in vitro, depending on the concentration and exposure time [7–9]: Apoptosis is induced by exposure to low concentrations of cisplatin (<50 μM) for a long time (<12 h), whereas necrosis is elicited by transient

Abbreviations: AMG, Methyl α-glucopyranoside; eNOS, endothelial nitric oxide synthase; FeTPPS, 5,10,15,20-tetrakis-(4-sulfonatophenyl)-porphyrinato iron (III); GSH, reduced glutathione; L-NAME, *N*-nitro-L-arginine methyl ester; OCTs, organic cation transporters; PI, propidium iodide; PKC, protein kinase C; PMA, phorbol 12-myristate 13-acetate; RNS, reactive nitrogen species; ROS, reactive oxygen species; TER, transepithelial electrical resistance; TJ, tight junction; ZO, zonula occludens

* Corresponding author. Department of Pharmaco-Biochemistry, School of Pharmaceutical Sciences, University of Shizuoka, 52-1 Yada, Shizuoka 422-8526, Japan. Tel.: +81 54 264 5674; fax: +81 54 264 5099.
E-mail address: ikari@u-shizuoka-ken.ac.jp (A. Ikari).

0005-2736/$ - see front matter © 2005 Elsevier B.V. All rights reserved.
doi:10.1016/j.bbamem.2005.10.003

exposure (<6 h) to higher concentrations (100–2000 μM). ROS generation, cytochrome *c* release from mitochondria, and caspase activation are involved in cisplatin-induced apoptosis [5,10,11]. Furthermore, protein kinase C (PKC) is implicated in cisplatin-induced caspase activation and apoptotic cell death [12,13]. In contrast, the cellular mechanisms underlying cisplatin-induced necrosis are not fully understood.

Four types of sodium-dependent glucose transporter family have been cloned, SGLT1, SGLT2, SGLT3, and NaGLT1. SGLT2 and NaGLT1 are expressed in the luminal membrane of the S1 segment and reabsorb the most filtered glucose. In contrast, SGLT1 is exclusively expressed in the S3 segment and reabsorbs the remaining glucose not reabsorbed in the early proximal tubule [14]. Besides glucose reabsorption, diverse physiological roles were found for the SGLT family: human SGLT1 functions as a water channel [15] and human SGLT3 functions as a glucose-sensitive sodium channel [16]. We recently found that SGLT1 is involved in the repair of plasma membrane integrity and tight junction (TJ) integrity injured by heat stress [17,18]. Interestingly, the diabetic state attenuates cisplatin nephrotoxicity in streptozotocin-induced diabetic rats [19]. In this rat model, the expression and glucose transport of SGLT1 are enhanced compared with control rats [20]. These reports assume that SGLT1 has a cytoprotective function against cisplatin injury.

The defining characteristics of epithelia include their ability to create selective barriers between tissue spaces and to generate polarity of the cellular structure and function. The most apical intercellular junction, the TJ, regulates barrier function by conferring size selectivity over paracellular transport. Many diseases of the kidney, such as ischemia/reperfusion or toxic injury, are closely related to the loss of the epithelial barrier [21,22]. This study was undertaken to examine the involvements of ROS and RNS in cisplatin-induced acute cell injury in renal proximal tubular epithelial cells. To determine cell injury, we measured transepithelial electrical resistance (TER), which is an easy functional parameter to monitor for epithelial monolayer integrity. Furthermore, we evaluated the effect of phloridzin, a potent SGLT1 inhibitor, on the TJ integrity, ROS and RNS generations and the cell death caused by cisplatin to determine the cytoprotective function of SGLT1.

2. Materials and methods

2.1. Cell Culture

Porcine renal epithelial LLC-PK_1 cells were obtained from JCRB (Tokyo, Japan). Cells were maintained in a humidified incubator at 37 °C in a 5% CO_2 atmosphere in Medium 199 (Sigma) supplemented with 10% fetal calf serum (FCS), 0.07 mg/ml penicillin G and 0.14 mg/ml streptomycin sulfate. The media contain 5.6 mM glucose. Cells were cultured for 24 h in the media without FCS before the experiments.

2.2. Measurement of TER

LLC-PK_1 cells were grown to confluent densities in a Transwell chamber (24-well plate, Corning Life Sciences, Acton, MA). TER was measured three times per well at indicated periods using a Millicell-ERS epithelial voltohmmeter (Millipore, Bedford, MA) and averaged values were collected. TER values (ohms × cm^2) were normalized by the area of the monolayer and calculated by subtracting the blank values from the filter and the bathing medium.

2.3. Measurement of necrotic and apoptotic dead cells

Cells were grown to sub-confluent and confluent densities on 35-mm glass-bottom culture dishes. The number of necrotic dead cells was measured using an annexin V-FITC apoptosis detection kit (Sigma, St. Louis, MO). The cells were incubated with cisplatin for indicated periods, and then incubated with annexin V-FITC and propidium iodide (PI) for 10 min at room temperature. Cells were washed twice with a binding buffer and visualized on an LSM 510 confocal laser microscope (Carl Zeiss, Germany) set with the appropriate filter for FITC (488 nm excitation and 505–530 nm emission filter) and PI detection (543 nm excitation and 650 nm emission filter). PI can penetrate into necrotic or late apoptotic cells, but not viable or early apoptotic cells, whereas in annexin V, a protein with high affinity for phosphatidylserine, can bind to exposed phospholipids in apoptotic cells [23]. The numbers of cells stained by only PI (necrotic dead cells) or only annexin V-FITC (apoptotic dead cells) were counted and expressed as a percentage of the total cell number.

2.4. SDS-polyacrylamide gel electrophoresis (SDS-PAGE) and Western blotting

Whole membrane fractions (40 μg) prepared from sub-confluent and confluent LLC-PK_1 cells were applied to the SDS-polyacrylamide gel. Proteins were blotted onto a PVDF membrane and incubated for 60 min with an anti-SGLT1 antibody followed by a peroxidase-conjugated anti-rabbit IgG. Finally, the blots were stained with ECL Western Blotting Detection Regents from Amersham Biosciences (Buckinghamshire, UK).

2.5. Extraction of LLC-PK1 cells with detergent solution

Confluent monolayers were rinsed three times with ice-cold PBS. Extractions were performed by overlaying the cells with 1 ml of CSK-1 buffer (0.5% Triton X-100, 100 mM NaCl, 10 mM Tris–HCl, pH 7.4, and 300 mM sucrose) containing a protease inhibitor cocktail (Sigma) plus 1 mM phenylmethylsulfonyl fluoride for 30 min at 4 °C on a gentle rocking platform. The extract was completely collected (Triton X-100 soluble fraction) and the residue (Triton X-100 insoluble fraction) was dissolved in a lysis buffer (1% Triton X-100, 150 mM NaCl, 1 mM EDTA, 20 mM Tris–HCl, pH 7.4, 0.1% SDS) containing protease inhibitors. These fractions were dissolved in sample buffer for SDS-PAGE. The protein concentration was measured using a protein assay kit (Bio-Rad Laboratories, CA) with bovine serum albumin as the standard.

2.6. Measurement of [^{14}C]-AMG uptake

Cells were grown to confluent densities on 24-well plates. Methyl α-glucopyranoside (AMG) was used as non-metabolic substrate of SGLT1. [^{14}C]-AMG uptake was assayed by incubating in a modified Hank's balanced salt solution (HBSS) containing 0.1 mM unlabeled AMG, 0.5 μCi/ml [^{14}C]-AMG (PerkinElemer Life and Analytical Sciences, Boston, MA), 137 mM NaCl, 5 mM KCl, 1 mM $CaCl_2$, 1 mM $MgCl_2$ and 10 mM HEPES (pH 7.4). After incubation for 30 min at 37 °C, the solution was aspirated quickly and washed with ice-cold HBSS without [^{14}C]-AMG four times. The cells were solubilized with 0.5 N NaOH and aliquots were taken to determine the radioactivity and protein concentration.

2.7. Immunofluorescence microscopy

The cells grown on a cover glass were washed twice with PBS supplemented with 0.5 mM $CaCl_2$ and 0.5 mM $MgCl_2$ prior to fixation with 10% formalin for 15 min at room temperature. The cells were then permeabilized with 0.2% Triton X-100 for 15 min, and incubated with PBS containing 5% skim milk (blocking solution) for 30 min. Incubation with the

anti-ZO-1 antibody (Zymed Laboratories, South San Francisco, CA) (final dilution 1/100) or the anti-endothelial nitric oxide synthase (eNOS) antibody (BIOMOL, Plymouth Meeting, PA) for 16 h at 4 °C was followed by washing three times with PBS, and they were then incubated for 90 min with the TexasRed-labeled anti-rabbit IgG (EY Laboratories, San Mateo, CA) in a blocking solution (dilution 1/100). Immunolabeled cells were visualized on the LSM 510 confocal microscope set with the appropriate filter for TexasRed (543 nm excitation and 650 nm emission filter). Images were further processed using Adobe Photoshop (Adobe System, Inc., San Jose, CA).

2.8. Measurement of intracellular ROS, RNS and nitric oxide productions

The intracellular formations of superoxide anion, peroxynitrite, and nitric oxide (NO) were detected using the fluorescent probes OxyBURST Green H_2DCFDA, H_2DCFDA (Molecular Probes, Eugene, OR) and DAF-2 DA (Daiichi Chemistry, Osaka, Japan), respectively. The cells grown on 96-well plates were incubated with HBSS containing 5 μM OxyBURST Green H_2DCFDA, 20 μM H_2DCFDA, or 5 μM DAF-2DA for 30 min at 37 °C. After washing twice with HBSS, the cells were exposed to cisplatin for the indicated periods. The fluorescence intensity of each probe was measured with excitation at 485 nm and emission at 538 nm using a Multilabel Counter 1420 ARVOsx (Perkin Elemer Life and Analytical Sciences).

2.9. Measurement of PKC activity

PKC activity was measured with a PKC assay kit (Promega, Madison, WI). The PepTag C1 peptide was used in the positive control assay. Cells were grown to confluent densities in 24-well plates and then exposed to cisplatin (500 μM) for 4 h. After washing twice with PBS, cells were scraped by a rubber policeman. After sonication, the samples were centrifuged at 1000×*g* for 5 min to remove the nuclear fraction. The supernatant was collected and the aliquot was used for the PKC assay. The assay was performed according to the manufacturer's instructions. In this assay, activated PKC increases the phosphorylated PepTag C1 peptides which migrate toward the anode by agarose gel electrophoresis.

2.10. Statistics

Results are presented as means ± S.E.M. Differences between groups were analyzed by one-way ANOVA, and corrections for multiple comparisons were made by Tukey's multiple comparison test. Comparisons between the two groups were made by the Student's *t* test. Significant differences were assumed at $P<0.05$.

3. Results

3.1. Inhibition of cisplatin-induced cell injury by SGLT1

LLC-PK_1, a well-differentiated epithelial cell line derived from porcine proximal tubule cells [24], has been utilized as a model system for studying the functions of polarized monolayer cells. Cisplatin (500 μM) decreased TER in a time-dependent manner (Fig. 1A). The cisplatin-induced TER

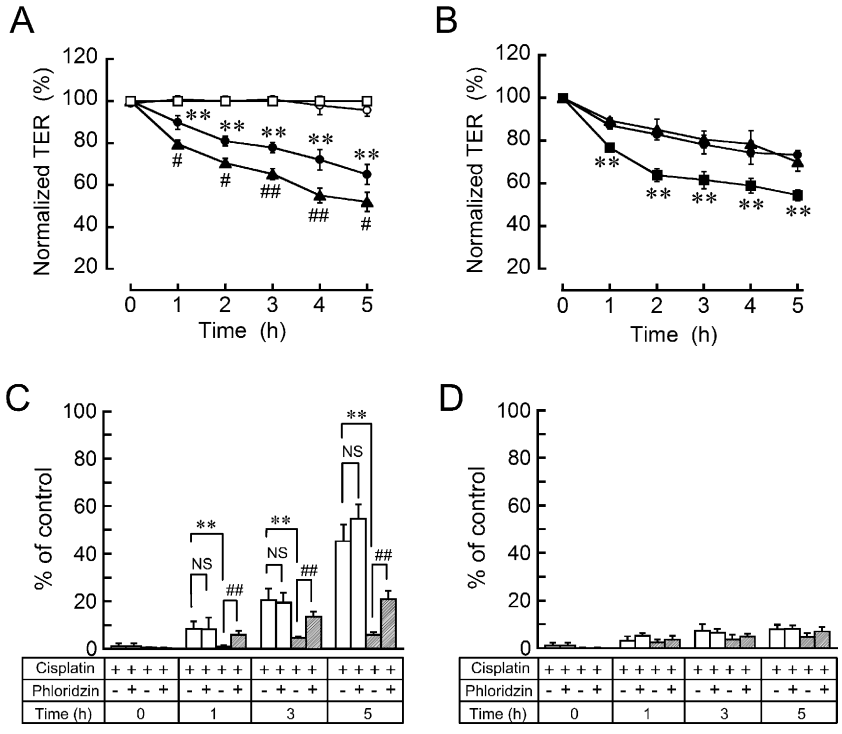

Fig. 1. Increases in transepithelial permeability and necrotic cell death by cisplatin. (A) LLC-PK_1 cells cultured on 24-transwell plates were incubated with 500 μM cisplatin (●), 100 μM phloridzin (□), or 500 μM cisplatin plus 100 μM phloridzin (▲). Control cells were incubated in the absence of these drugs (○). TER was measured at the indicated periods. Each TER values were normalized to the TER value at 0 h. The average TER value of control LLC-PK_1 cells was 78.4 ± 2.2 ohms × cm^2 ($n=6$). *$P<0.05$ and **$P<0.01$, significantly different from control. $^{\#}P<0.05$ and $^{\#\#}P<0.01$, significantly different from cisplatin alone. (B) Cells were incubated with 500 μM cisplatin (●), 500 μM cisplatin plus 10 μM cytochalasin B (▲), or 500 μM cisplatin plus 100 μM phloretin (■) ($n=4$–6). **$P<0.01$, significantly different from cisplatin alone. (C and D) Cells were cultured at sub-confluent (open columns) and confluent densities (hatched columns) on glass-bottom culture dishes. Cells were preincubated with 500 μM cisplatin or 500 μM cisplatin plus 100 μM phloridzin for the indicated periods prior to loading with PI and annexin V-FITC. The numbers of necrotic dead cells stained by only PI (C) or apoptotic dead cells stained by only annexin V-FITC (D) were counted, and then expressed as a percentage of the total cell number ($n=6$). NS, not significantly different from the value without phloridzin. **$P<0.01$, significantly different from the value in the sub-confluent densities. $^{\#\#}P<0.01$ significantly different from the value without phloridzin.

decrease was significantly accelerated by phloridzin (100 μM), a potent SGLT1 inhibitor. Phloridzin alone did not change the basal TER. Phloretin, a nonselective inhibitor of SGLT and a facilitate glucose transporter (GLUT), enhanced TER decrease caused by cisplatin, whereas cytochalasin B, a selective GLUT inhibitor, had no effect on TER decrease (Fig. 1B). These results indicate that cisplatin increases in the TJ permeability and SGLT1 partially blocks it. As shown in Fig. 1C, cisplatin increased the number of necrotic dead cells. The degree of dead cells in the sub-confluent densities was higher than that in the confluent densities. Phloridzin significantly enhanced the necrotic dead cells caused by cisplatin only in the confluent densities. The cisplatin-induced TER decrease corresponded to the increase in necrotic dead cells. On the other hand, the number of apoptotic dead cells was not affected by treatment of cisplatin and phloridzin for 5 h (Fig. 1D). Phloridzin alone did not increase in the necrotic and apoptotic dead cells (data not shown). These results indicate that high doses of cisplatin increase the transepithelial permeability and necrotic dead cells in a short period, and that SGLT1 endogenously protects cells from the cisplatin-induced injury.

3.2. Effects of cisplatin on the expression and glucose transport of SGLT1

After the formation of a confluent monolayer, LLC-PK$_1$ cells form the TJ and express SGLT1 at the apical surface [25]. In western blotting, the specific band of SGLT1 appeared at about 70 kDa in the confluent densities (Fig. 2A). Cisplatin had no effect on SGLT1 expression for 5 h (Fig. 2B). LLC-PK$_1$ cells also express SGLT3, but sodium-dependent glucose transport is mainly mediated by SGLT1 [26]. Phloridzin-sensitive [^{14}C]-AMG uptake was significantly increased after developing cell confluence in agreement with the expression of SGLT1 protein (Fig. 2C). Cisplatin had no effect on [^{14}C]-AMG uptake for 5 h (Fig. 2D). Both SGLT1 protein expression and [^{14}C]-AMG uptake disappeared after 24-h treatment of cisplatin. These results indicate that SGLT1 transports glucose into the cells during the 5 h of cisplatin treatment in spite of the increase in the transepithelial permeability and the glucose uptake may be involved in the protection against cell injury caused by cisplatin.

3.3. Increases in intracellular RNS and ROS productions by cisplatin

Cells were loaded with DAF-2DA to measure intracellular NO production in real-time. NO production was significantly increased by cisplatin within 1 h and continued to rise over the 5-h period (Fig. 3A). Phloridzin has no effect on the basal and cisplatin-induced NO production. The expression of eNOS proteins have been reported in the renal cortex and medulla of the rat [27], and we identified their expression in the LLC-PK$_1$ cells by Western blotting (data not shown). The localization of eNOS within the cells influences NO production [28]. In immunofluorescence measurements, cisplatin translocated eNOS from the cytosolic compartments to the plasma

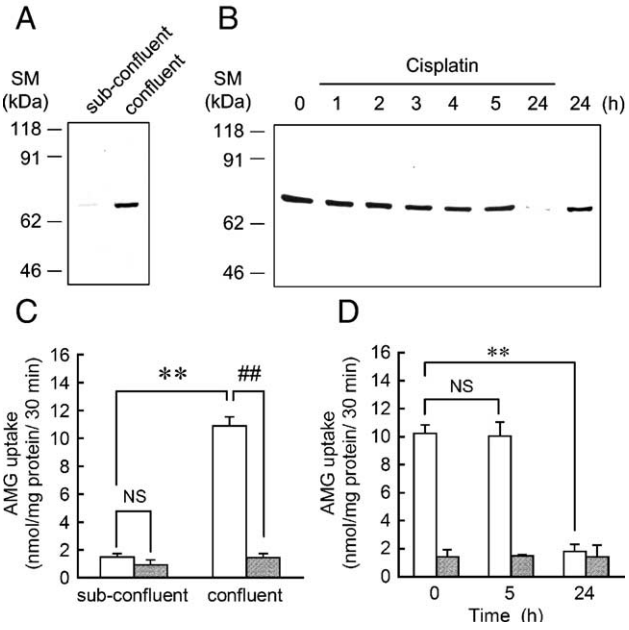

Fig. 2. Effects of cisplatin on SGLT1 expression and [^{14}C]-AMG uptake. (A) Cells were cultured at sub-confluent or confluent densities. Whole membrane fractions (40 μg) were run on 10% SDS-polyacrylamide gels and transferred to the PVDF membrane. The membrane was immunoblotted with the anti-SGLT1 antibody. The specific band of SGLT1 was observed at about 70 kDa. (B) Cells were preincubated with or without 500 μM cisplatin for the indicated periods. Whole membrane fractions (40 μg) were run on 10% SDS-polyacrylamide gels and then blotted with the anti-SGLT1 antibody. (C) Cells were cultured at sub-confluent or confluent densities on a 24-well plate. [^{14}C]-AMG uptake was carried out at 37 °C for 30 min in the presence (hatched columns) or absence (open columns) of 100 μM phloridzin (n=6). NS, not significantly different from the value without phloridzin. **P<0.01, significantly different from the value in the sub-confluent densities. $^{\#\#}P$<0.01, significantly different from the value without phloridzin. (D) Cells were preincubated with 500 μM cisplatin for 5 h or 24 h in the confluent densities. [^{14}C]-AMG uptake was carried out at 37 °C for 30 min in the presence (hatched columns) or absence (open columns) of 100 μM phloridzin (n=4–6). NS, not significantly different from the value at 0 h. **P<0.01, significantly different from the value at 0 h.

membrane (Fig. 3B), indicating that cisplatin increased intracellular NO production mediated via eNOS translocation. Next, we examined the productions of superoxide anion and peroxynitrite using OxyBURST Green H$_2$DCFDA and H$_2$DCFDA, respectively. Cisplatin increased superoxide anion and peroxynitrite productions in a time-dependent manner (Fig. 3C and D). Phloridzin enhanced cisplatin-induced peroxynitrite production, whereas it had no effect on cisplatin-induced superoxide anion production. The basal productions of superoxide anion and peroxynitrite were not changed by phloridzin alone, the same as NO production. These results suggest that cisplatin increases in RNS and ROS productions in a time-dependent manner and SGLT1 endogenously suppresses the intracellular accumulation of peroxynitrite caused by cisplatin.

3.4. Disruption of the TJ structure by cisplatin

The TJ consists of a number of proteins including occludin, claudins, zonula occludens-1 (ZO-1), ZO-2, and cingulin [29,30]. ZO-1 has an important role in the cross-links between

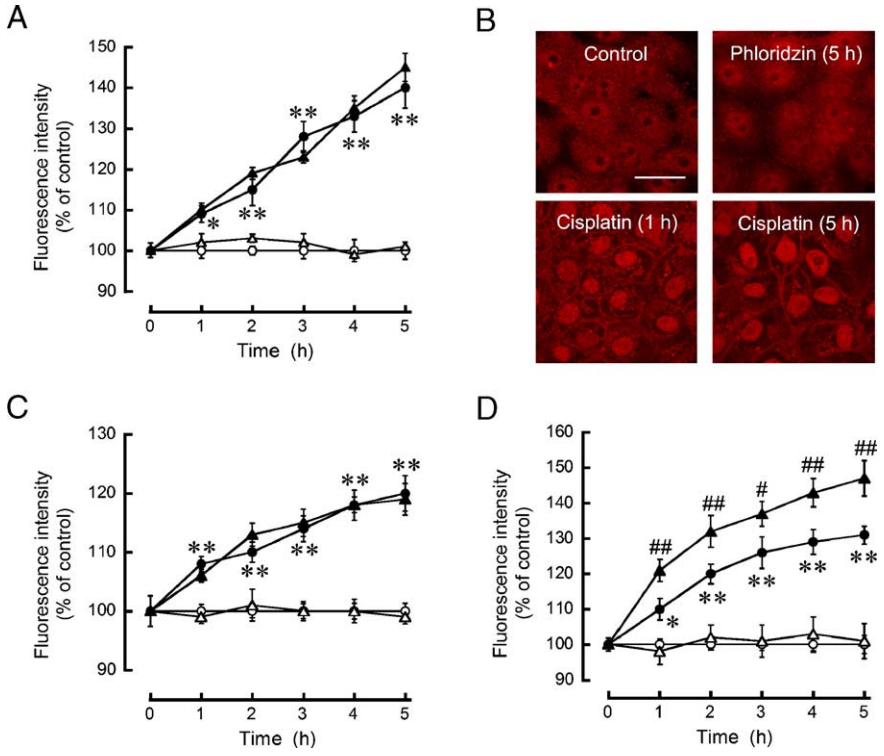

Fig. 3. Inhibition of cisplatin-induced peroxynitrite production by SGLT1. (A, C, and D) Cells were cultured at confluent densities on a 96-well plate prior to loading with 5 μM DAF-2DA (A), 5 μM OxyBURST Green H_2DCFDA (C), or 20 μM H_2DCFDA (D) for 30 min at 37 °C. Then, cells were incubated with (closed symbols) or without 500 μM cisplatin (open symbols) in the presence (triangles) or absence (circles) of 100 μM phloridzin for the indicated periods. The fluorescence intensity was sequentially measured with excitation at 485 nm and emission at 538 nm ($n=8$). (B) Cells were cultured at confluent densities on a cover glass. Then, cells were preincubated with 500 μM cisplatin or 100 μM phloridzin for the indicated periods. After fixation with formalin, the cells were incubated with the anti-eNOS antibody prior to incubation with the TexasRed-labeled anti-rabbit IgG. Immunolabeled cells were visualized on the LSM 510 confocal microscope (Scale bar=10 μm).

TJ strands and the actin-based cytoskeleton. ZO-1 was localized at the lateral surface of the plasma membrane in LLC-PK_1 cells (Fig. 4A). The localization of ZO-1 in the cell–cell contact area was abolished by cisplatin. The cisplatin-induced internalization of ZO-1 protein was inhibited by *N*-nitro-L-arginine methyl ester (L-NAME, 100 μM), a NOS inhibitor. The qualitative change in the ZO-1 distribution pattern likely represents an alteration in the association of ZO-1 with the actin-based cytoskeleton. Treatment with cisplatin or cisplatin plus L-NAME did not change the total amount of ZO-1 (Fig. 4B). However, ZO-1 became more soluble to the Triton X-100-containing buffer by cisplatin. L-NAME inhibited the detergent extraction of ZO-1 caused by cisplatin. Similarly, the decrease in TER by cisplatin was inhibited by L-NAME (Fig. 4C). These results indicate that cisplatin disrupts the TJ structure mediated by NO production.

3.5. Effect of PKC inhibitor on cisplatin-induced injury

The atypical PKC isoform αPKC is localized at the cell junctional complex in LLC-PK_1 cells and PKC-activating phorbol esters induce an increase in TJ permeability [31]. We also observed that phorbol 12-myristate 13-acetate (PMA), an activator of PKC, decreased in TER in LLC-PK_1 cells (Fig. 5A). The PMA-induced TER decrease was completely blocked by calphostin C, a PKC inhibitor. PKC inhibitors protect against cisplatin-induced apoptosis in LLC-PK_1 cells [13], which is associated with protection against the loss of cell–cell contact. However, the high doses of cisplatin-induced TER decrease were not blocked by calphostin C (Fig. 5B). Cotreatment of cisplatin with PMA led to an additive TER decrease. Control activated PKC increases of phosphorylated PepTag C1 peptides which migrate toward the anode (Fig. 5C). PepTag C1 peptides, however, migrated toward the cathode in the control and the cisplatin-treated cells. Furthermore, calphostin C blocked the PMA-induced internalization of ZO-1, but did not block the cisplatin-induced internalization of ZO-1 (Fig. 5D). These results indicate that PKC is not involved in the disruption of the TJ structure by high doses of cisplatin.

3.6. Involvement of peroxynitrite in cisplatin-induced injury

The toxicity of NO is enhanced by its reaction with superoxide to form peroxynitrite, which induces lipid peroxidation [32]. In rats treated with cisplatin, peroxynitrite has been suggested to be involved in cisplatin-induced nephrotoxicity, but its target is unknown [33]. To eliminate intracellular peroxynitrite, we used two types of drugs: 5,10,15,20-tetrakis-(4-sulfonatophenyl)-porphyrinato iron (III) (FeTPPS), a peroxynitrite decomposition catalyst, and reduced glutathione (GSH), a peroxynitrite scavenger. The cisplatin-

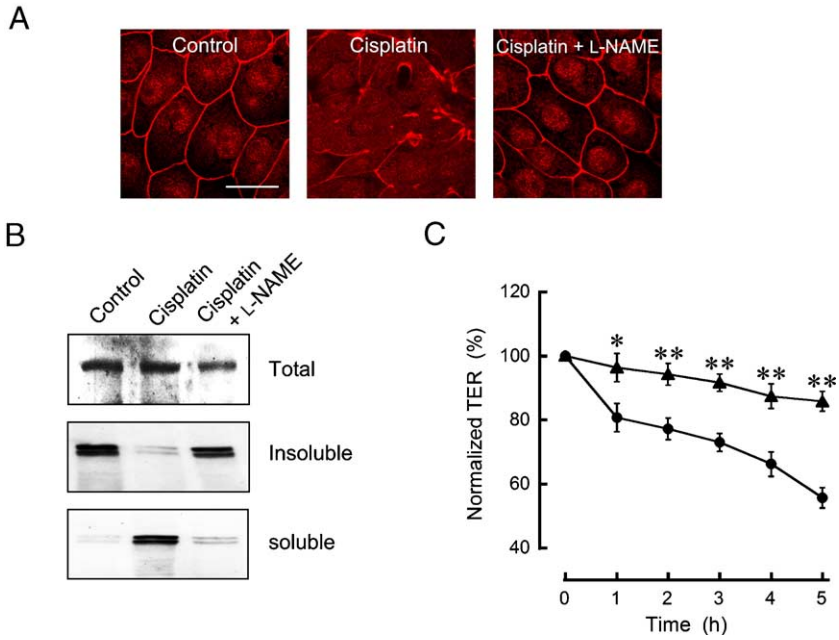

Fig. 4. Effect of L-NAME on cisplatin-induced ZO-1 internalization. (A) Cells were cultured at confluent densities on a cover glass. Then, cells were preincubated with 500 μM cisplatin for 5 h in the presence or absence of 100 μM L-NAME. After fixation with formalin, the cells were incubated with the anti-ZO-1 antibody prior to incubation with the TexasRed-labeled anti-rabbit IgG (Scale bar = 10 μm). (B) Cells were incubated with 500 μM cisplatin for 5 h in the presence or absence of 100 μM L-NAME. Whole membrane (40 μg), Triton X-100 soluble (80 μg), and Triton X-100 insoluble (40 μg) fractions were run on 7.5% SDS-polyacrylamide gels and transferred to the PVDF membrane. The membrane was immunoblotted with the anti-ZO-1 antibody. The specific band of ZO-1 was observed at about 220 kDa. (C) Cells were incubated on 24-transwell plates for 0–5 h in the presence of 500 μM cisplatin (●) or 500 μM cisplatin plus 100 μM L-NAME (▲). TER was measured at the indicated periods ($n = 6$). *$P < 0.05$ and **$P < 0.01$, significantly different from the value without L-NAME.

induced internalization and detergent extraction of ZO-1 were inhibited by FeTPPS and GSH (Fig. 6A and B). These drugs significantly inhibited the cisplatin-induced TER decrease (Fig. 6C). These results are consistent with the effect of L-NAME (Fig. 4). Furthermore, FeTPPS and GSH significantly decreased the number of necrotic dead cells caused by cisplatin without affecting apoptotic dead cells (Fig. 6D). Our data suggest that peroxynitrite is a key mediator in the high doses of cisplatin-induced TJ disruption and necrotic cell death.

4. Discussion

In cisplatin chemotherapy, nephrotoxicity is a major adverse effect that limits its use at higher doses to maximize its therapeutic effect. Several mechanisms are implicated in the dose-dependent and cumulative cisplatin-induced nephrotoxic injury. Exposure of cells to substantially lower concentrations (<50 μM) for several days leads to apoptosis [7–9]. On the other hand, high concentrations of cisplatin (100–2000 μM) lead to cell necrosis over several hours. Cisplatin actively accumulates in proximal tubular epithelial cells [34]. However, the mechanism by which high doses of cisplatin cause renal damage remains unclear. In this study, we found that cisplatin increased in the transepithelial permeability and necrotic dead cells in LLC-PK_1 cells (Fig. 1).

In proximal tubular epithelial cells, cisplatin may be transported into the cytosol, mediated by organic cation transporters (OCTs) [35], and then be excreted into urine, mediated by an unknown pathway. High expression levels of OCTs can be found in the S3 segment of the proximal tubule [36]. The epithelial cells must have a cytoprotective function against cisplatin to excrete high doses of cisplatin. SGLT1 is predominantly expressed in the S3 segment and reabsorbs the remaining glucose not reabsorbed in the early proximal tubule. In LLC-PK_1 cells, SGLT1 appeared after the confluent densities (Fig. 2). Interestingly, the protective function of cells against high doses of cisplatin was more potent in the confluent densities than in the sub-confluent densities (Fig. 1C). We suggest that the function and morphology of LLC-PK_1 cells are changed by differentiation, and SGLT1 expression is partially related to the acquisition of a protective function against cisplatin.

Cisplatin inhibits the low-affinity SGLT (probably SGLT2) in renal proximal tubular cells [37] and in brush border membrane vesicles prepared from the renal cortex of animals exposed to cisplatin in vivo [38]. The cisplatin-induced inhibition of SGLT2 may result from a direct interaction between cisplatin and the SGLT2 protein. In the present study, a high affinity SGLT (SGLT1) was not inhibited by cisplatin for at least 5 h (Fig. 2). Potdevin et al. [39] reported that cisplatin-induced inhibition of SGLT2 could result from covalent platinum binding to SH groups of the transporter. The amino acid sequence of human SGLT2 is 59% identical to that of human SGLT1 [40]. The cysteine residues of SGLT2 at 535, 546, 592, and 610 are not conserved in SGLT1. We suggest that SGLT1 fulfills its function even under the exposure of cells to cisplatin.

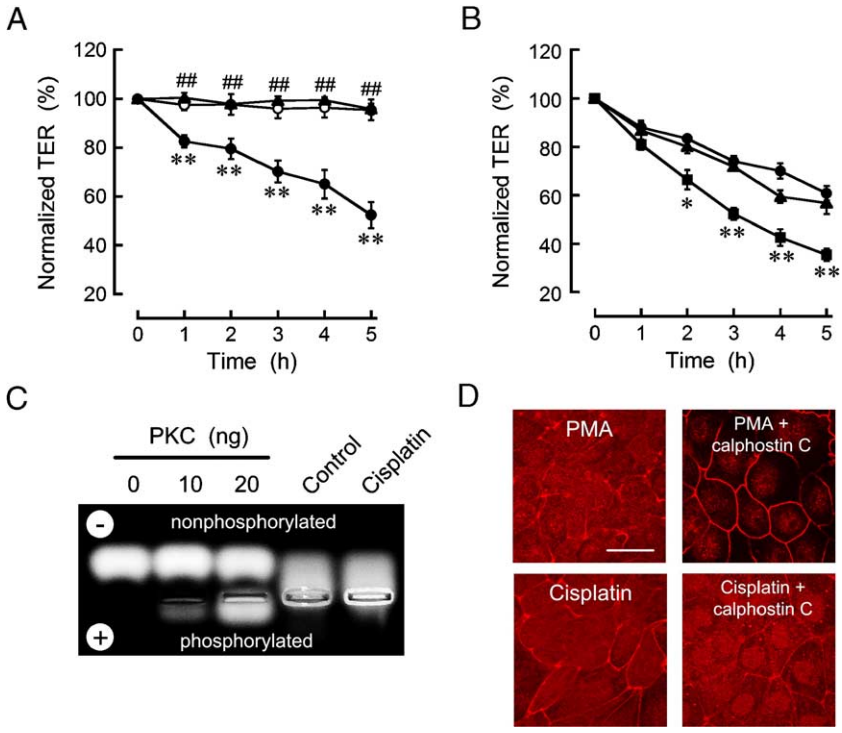

Fig. 5. Independency of PKC on the increase in transepithelial permeability by cisplatin. (A) Cells were incubated with 100 nM PMA (●) or 100 nM PMA plus 500 nM calphostin C (▲). Control cells were incubated in the absence of these drugs (○). TER was measured at the indicated periods ($n=6$). $^{**}P<0.01$, significantly different from control. $^{\#\#}P<0.01$, significantly different from PMA alone. (B) Cells were incubated with 500 μM cisplatin (●), 500 μM cisplatin plus 500 nM calphostin C (▲), or 500 μM cisplatin plus 100 nM PMA (■). TER was measured at the indicated periods ($n=4–6$). (C) Cells were incubated on 24-well plates for 4 h in the presence or absence of 500 μM cisplatin. After the scraping and sonication of cells, the supernatant without the nuclear fraction was collected by centrifugation. An aliquot (100 μg) was used for the PKC assay. As a positive control assay, PKC (control enzyme) was added at 10 or 20 ng. (D) Cells were preincubated with 100 nM PMA, 100 nM PMA plus 500 nM calphostin C, 500 μM cisplatin, or 500 μM cisplatin plus 500 nM calphostin C for 5 h. After fixation with formalin, the cells were incubated with the anti-ZO-1 antibody prior to the incubation with the TexasRed-labeled anti-rabbit IgG (Scale bar=10 μm).

Glucose uptake is involved in the cytoprotective function against hydrogen peroxide [41] and the inhibition of mitochondrial respiration [42]. The general effects of glucose may be mediated by the uptake and subsequent intracellular metabolism of glucose. GSH can counteract the damaging effects of ROS and RNS. Actually, the addition of GSH suppressed the cisplatin-induced TER decrease and ZO-1 internalization (Fig. 6). GSH is the substrate for glutathione peroxidase, converting GSH to its oxidized disulfide form (GSSG). GSH can be regenerated from GSSG by glutathione reductase, which uses NADPH produced mainly by glucose metabolism via the pentose phosphate cycle. One of the cytoprotective mechanisms of SGLT1 may be the reduction of RNS by glucose metabolism. Phloridzin enhanced the cisplatin-induced TER decrease (Fig. 1), whereas it did not enhance the cisplatin-induced NO and superoxide anion productions (Fig. 3A and D). Furthermore, the inhibition of GLUT by cytochalasin B did not affect the cisplatin-induced TER decrease. These results suggest that glucose transported by SGLT1 suppresses peroxynitrite production or incites peroxynitrite metabolite without inhibiting cisplatin-induced NO and superoxide anion productions.

NO is able to react with superoxide to produce peroxynitrite, which is a powerful oxidant, being more reactive than its precursors. The administration of N^{G}-nitro-L-arginine methyl ester, an inhibitor of NOS, reduced nephrotoxicity and also decreased the content of blood urea nitrogen in cisplatin-treated rats [43]. Cisplatin-induced nephrotoxicity was attenuated by FeTPPS, suggesting the involvement of peroxynitrite [33]. It is, however, unknown how peroxynitrite damages the proximal tubular cells. We found that the cisplatin-induced TER decrease was inhibited by L-NAME, FeTPPS, and GSH (Figs. 4 and 6). Furthermore, these drugs prevented the cisplatin-induced disruption of ZO-1 localization at TJ and changes in the detergent solubility of ZO-1. Peroxynitrite produced by cisplatin must be involved in the disruption of TJ structure.

In cultured epithelial cells, the disassembly of ZO-1 from TJ strands correlates with disruption of the epithelial barrier [44,45]. In calcium switch experiments, low extracellular calcium leads to a decline in TER and the internalization or diffusion of TJ proteins [46]. ZO-1 becomes more soluble with detergent-containing solutions, suggesting a weakening of the interactions between ZO-1 and the cytoskeleton. Oxidative stress also leads to the decline of TER and the disruption of ZO-1 localization at TJ [47]. In cisplatin-induced apoptosis, PKC is suggested to be involved in the loss of adherens junctions in LLC-PK_1 cells [13]. There is a possibility that high doses of cisplatin disrupt TJ structure mediated via PKC activation. However, cisplatin did not activate PKC and the cisplatin-induced TER decrease was not inhibited by the PKC inhibitor (Fig. 5). Furthermore, cotreatment of cisplatin with PMA accelerated the TER decrease compared with cisplatin

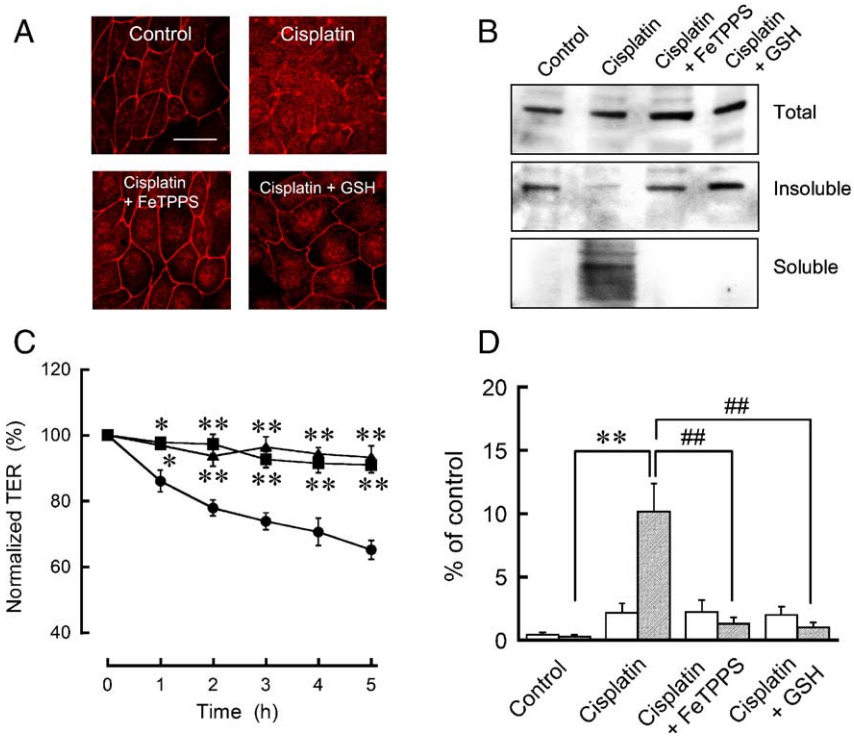

Fig. 6. Inhibition of cisplatin-induced TJ disruption by peroxynitrite inhibitors. (A) Cells were incubated with 500 μM cisplatin for 5 h in the presence or absence of 50 μM FeTPPS or 100 μM GSH. After fixation with formalin, the cells were incubated with the anti-ZO-1 antibody prior to incubation with the TexasRed-labeled anti-rabbit IgG (Scale bar=10 μm). (B) Cells were incubated with 500 μM cisplatin for 5 h in the presence or absence of 50 μM FeTPPS or 100 μM GSH. Whole membrane (40 μg), Triton X-100 soluble (80 μg), and Triton X-100 insoluble (40 μg) fractions were run on 7.5% SDS-polyacrylamide gels and transferred to the PVDF membrane. The membrane was immunoblotted with the anti-ZO-1 antibody. (C) Cells were incubated with 500 μM cisplatin (●), 500 μM cisplatin plus 50 μM FeTPPS (▲), or 500 μM cisplatin plus 100 μM GSH (■). TER was measured at the indicated periods ($n=6$). *$P<0.05$ and **$P<0.01$, significantly different from cisplatin alone. (D) Cells were preincubated with 500 μM cisplatin for 5 h in the presence or absence of 50 μM FeTPPS or 100 μM GSH prior to loading with PI and annexin V-FITC. Necrotic dead cells (hatched columns) and apoptotic dead cells (open columns) were expressed as a percentage of the total cell number ($n=6$). **$P<0.01$, significantly different from control. $^{\#\#}P<0.01$, significantly different from cisplatin alone.

alone. Clarke et al. [31] reported that PKC activation leads to a decline in TER, but it did not change the detergent solubility of ZO-1. However, ZO-1 became more soluble to the Triton X-100-containing solution by cisplatin (Fig. 4). We suggest that PKC is not involved in high doses of cisplatin-induced TJ injury.

In conclusion, high doses of cisplatin cause nephrotoxicity mediated via a different pathway from that in apoptosis. Cisplatin increases intracellular peroxynitrite production, resulting in the disruption of TJ construction in renal proximal tubular epithelial cells. The disruption of barrier function and the loss of polarity must lead to tissue injury. SGLT1 expressed in the S3 segment partially suppresses cisplatin-induced peroxynitrite production and protects cells from cisplatin-induced nephrotoxicity. In the animal model, tubular injury plays a central role in the reduction of the glomerular filtration rate in acute tubular necrosis. In cisplatin chemotherapy, the elimination of peroxynitrite may be useful in arresting the development of nephrotoxicity.

Acknowledgements

We thank Dr. Julia E. Lever (University of Texas Medical School, Houston, USA) for providing a rabbit polyclonal antibody raised porcine SGLT1. This work was supported in part by a Grant-in-Aid for Encouragement of Young Scientists from the Ministry of Education, Science, Sports and Culture of Japan.

References

[1] A.G. Basnakian, E.O. Apostolov, X. Yin, M. Napirei, H.G. Mannherz, S.V. Shah, Cisplatin nephrotoxicity is mediated by deoxyribonuclease I, J. Am. Soc. Nephrol. 16 (2005) 697–702.
[2] R. Safirstein, J. Winston, M. Goldstein, D. Moel, S. Dikman, J. Guttenplan, Cisplatin nephrotoxicity, Am. J. Kidney Dis. 8 (1986) 356–367.
[3] D.C. Dobyan, J. Levi, C. Jacobs, J. Kosek, M.W. Weiner, Mechanism of cis-platinum nephrotoxicity: II. Morphologic observations, J. Pharmacol. Exp. Ther. 213 (1980) 551–556.
[4] A.E. Vickers, K. Rose, R. Fisher, M. Saulnier, P. Sahota, P. Bentley, Kidney slices of human and rat to characterize cisplatin-induced injury on cellular pathways and morphology, Toxicol. Pathol. 32 (2004) 577–590.
[5] S.M. Baek, C.H. Kwon, J.H. Kim, J.S. Woo, J.S. Jung, Y.K. Kim, Differential roles of hydrogen peroxide and hydroxyl radical in cisplatin-induced cell death in renal proximal tubular epithelial cells, J. Lab. Clin. Med. 142 (2003) 178–186.
[6] A.J. Anand, B. Bashey, Newer insights into cisplatin nephrotoxicity, Ann. Pharmacother. 27 (1993) 1519–1525.
[7] B.S. Cummings, R.G. Schnellmann, Cisplatin-induced renal cell apoptosis: caspase 3-dependent and -independent pathways, J. Pharmacol. Exp. Ther. 302 (2002) 8–17.
[8] A.H. Lau, Apoptosis induced by cisplatin nephrotoxic injury, Kidney Int. 56 (1999) 1295–1298.

[9] W. Lieberthal, V. Triaca, J. Levine, Mechanisms of death induced by cisplatin in proximal tubular epithelial cells: apoptosis vs. necrosis, Am. J. Physiol. 270 (1996) F700–F708.
[10] H.R. Brady, B.C. Kone, M.E. Stromski, M.L. Zeidel, G. Giebisch, S.R. Gullans, Mitochondrial injury: an early event in cisplatin toxicity to renal proximal tubules, Am. J. Physiol. 258 (1990) F1181–F1187.
[11] G.P. Kaushal, V. Kaushal, X. Hong, S.V. Shah, Role and regulation of activation of caspases in cisplatin-induced injury to renal tubular epithelial cells, Kidney Int. 60 (2001) 1726–1736.
[12] G. Nowak, Protein kinase C-alpha and ERK1/2 mediate mitochondrial dysfunction, decreases in active Na+ transport, and cisplatin-induced apoptosis in renal cells, J. Biol. Chem. 277 (2002) 43377–43388.
[13] R. Imamdi, M. de Graauw, B. van de Water, Protein kinase C mediates cisplatin-induced loss of adherens junctions followed by apoptosis of renal proximal tubular epithelial cells, J. Pharmacol. Exp. Ther. 311 (2004) 892–903.
[14] W.S. Lee, Y. Kanai, R.G. Wells, M.A. Hediger, The high affinity Na+/glucose cotransporter. Re-evaluation of function and distribution of expression, J. Biol. Chem. 269 (1994) 12032–12039.
[15] P.P. Duquette, P. Bissonnette, J.Y. Lapointe, Local osmotic gradients drive the water flux associated with Na+/glucose cotransport, Proc. Natl. Acad. Sci. U. S. A. 98 (2001) 3796–3801.
[16] A. Diez-Sampedro, B.A. Hirayama, C. Osswald, V. Gorboulev, K. Baumgarten, C. Volk, E.M. Wright, H. Koepsell, A glucose sensor hiding in a family of transporters, Proc. Natl. Acad. Sci. U. S. A. 100 (2003) 11753–11758.
[17] A. Ikari, M. Nakano, M. Ishibashi, K. Kawano, Y. Suketa, H. Harada, K. Takagi, Recovery from heat shock injury by activation of Na+-glucose cotransporter in renal epithelial cells, Biochim. Biophys. Acta 1643 (2003) 47–53.
[18] A. Ikari, M. Nakano, Y. Suketa, H. Harada, K. Takagi, Reorganization of ZO-1 by sodium-dependent glucose transporter activation after heat stress in LLC-PK1 cells, J. Cell. Physiol. 203 (2005) 471–478.
[19] L.A. Scott, E. Madan, M.A. Valentovic, Attenuation of cisplatin nephrotoxicity by streptozotocin-induced diabetes, Fundam. Appl. Toxicol. 12 (1989) 530–539.
[20] E.S. Debnam, M.W. Smith, P.A. Sharp, S.K. Srai, A. Turvey, S.J. Keable, The effects of streptozotocin diabetes on sodium-glucose transporter (SGLT1) expression and function in rat jejunal and ileal villus-attached enterocytes, Pflugers Arch. 430 (1995) 151–159.
[21] H. Hagar, N. Ueda, S.V. Shah, Role of reactive oxygen metabolites in DNA damage and cell death in chemical hypoxic injury to LLC-PK_1 cells, Am. J. Physiol. 271 (1996) F209–F215.
[22] G. Nowak, M.D. Aleo, J.A. Morgan, R.G. Schnellmann, Recovery of cellular functions following oxidant injury, Am. J. Physiol. 274 (1998) F509–F515.
[23] G. Koopman, C.P. Reutelingsperger, G.A. Kuijten, R.M. Keehnen, S.T. Pals, M.H. van Oers, Annexin V for flow cytometric detection of phosphatidylserine expression on B cells undergoing apoptosis, Blood 84 (1994) 1415–1420.
[24] R.N. Hull, W.R. Cherry, G.W. Weaver, The origin and characteristics of a pig kidney cell strain, LLC-PK, In Vitro 12 (1976) 670–677.
[25] J.M. Mullin, J. Weibel, L. Diamond, A. Kleinzeller, Sugar transport in the LLC-PK1 renal epithelial cell line: similarity to mammalian kidney and the influence of cell density, J. Cell. Physiol. 104 (1980) 375–389.
[26] C.A. Rabito, D.A. Ausiello, Na+-dependent sugar transport in a cultured epithelial cell line from pig kidney, J. Membr. Biol. 54 (1980) 31–38.
[27] B.C. Kone, C. Baylis, Biosynthesis and homeostatic roles of nitric oxide in the normal kidney, Am. J. Physiol. 272 (1997) F561–F578.
[28] T. Michel, Targeting and translocation of endothelial nitric oxide synthase, Braz. J. Med. Biol. Res. 32 (1999) 1361–1366.
[29] S. Tsukita, M. Furuse, M. Itoh, Structural and signalling molecules come together at tight junctions, Curr. Opin. Cell Biol. 11 (1999) 628–633.
[30] J.M. Anderson, C.M. Van Itallie, Tight junctions and the molecular basis for regulation of paracellular permeability, Am. J. Physiol. 269 (1995) G467–G475.
[31] H. Clarke, A.P. Soler, J.M. Mullin, Protein kinase C activation leads to dephosphorylation of occludin and tight junction permeability increase in LLC-PK_1 epithelial cell sheets, J. Cell Sci. 113 (2000) 3187–3196.
[32] V.M. Darley-Usmar, N. Hogg, V.J. O'Leary, M.T. Wilson, S. Moncada, The simultaneous generation of superoxide and nitric oxide can initiate lipid peroxidation in human low density lipoprotein, Free Radic. Res. Commun. 17 (1992) 9–20.
[33] Y.I. Chirino, R. Hernández-Pando, J. Pedraza-Chaverrí, Peroxynitrite decomposition catalyst ameliorates renal damage and protein nitration in cisplatin-induced nephrotoxicity in rats, BMC Pharmacol. 4 (2004) 20.
[34] M.K. Kuhlmann, G. Burkhardt, H. Köhler, Insights into potential cellular mechanisms of cisplatin nephrotoxicity and their clinical application, Nephrol. Dial. Transplant. 12 (1997) 2478–2480.
[35] T. Ludwig, C. Riethmüller, M. Gekle, G. Schwerdt, H. Oberleithner, Nephrotoxicity of platinum complexes is related to basolateral organic cation transport, Kidney Int. 66 (2004) 196–202.
[36] Y. Urakami, M. Okuda, S. Masuda, M. Akazawa, H. Saito, K. Inui, Distinct characteristics of organic cation transporters, OCT1 and OCT2, in the basolateral membrane of renal tubules, Pharm. Res. 18 (2001) 1528–1534.
[37] F. Courjault-Gautier, C. Le Grimellec, M.C. Giocondi, H.J. Toutain, Modulation of sodium-coupled uptake and membrane fluidity by cisplatin in renal proximal tubular cells in primary culture and brush-border membrane vesicles, Kidney Int. 47 (1995) 1048–1056.
[38] M. Yanase, O. Uyama, T. Nakanishi, N. Shiratsuki, M. Sugita, Decreased sodium dependent D-glucose transport across renal brush-border membranes in cis-diamminedichloride platinum induced acute renal failure, Ren. Fail. 14 (1992) 23–30.
[39] S. Potdevin, F. Courjault-Gautier, B.M. Du Sorbier, P. Ripoche, H.J. Toutain, Role of protein thiols in inhibition of sodium-coupled glucose uptake by cisplatin in renal brush-border membrane vesicles, J. Pharmacol. Exp. Ther. 284 (1998) 142–150.
[40] R.G. Wells, A.M. Pajor, Y. Kanai, E. Turk, E.M. Wright, M.A. Hediger, Cloning of a human kidney cDNA with similarity to the sodium-glucose cotransporter, Am. J. Physiol. 263 (1992) F459–F465.
[41] S. Lord-Fontaine, D.A. Averill-Bates, Heat shock inactivates cellular antioxidant defenses against hydrogen peroxide: protection by glucose, Free Radic. Biol. Med. 32 (2002) 752–765.
[42] P. Cidad, A. Almeida, J.P. Bolaños, Inhibition of mitochondrial respiration by nitric oxide rapidly stimulates cytoprotective GLUT3-mediated glucose uptake through 5′-AMP-activated protein kinase, Biochem. J. 384 (2004) 629–636.
[43] R.C. Srivastava, A. Farookh, N. Ahmad, M. Misra, S.K. Hasan, M.M. Husain, Evidence for the involvement of nitric oxide in cisplatin-induced toxicity in rats, Biometals 9 (1996) 139–142.
[44] M.L. Chen, C. Pothoulakis, J.T. LaMont, Protein kinase C signaling regulates ZO-1 translocation and increased paracellular flux of T84 colonocytes exposed to Clostridium difficile toxin A, J. Biol. Chem. 277 (2002) 4247–4254.
[45] A. Youakim, M. Ahdieh, Interferon-gamma decreases barrier function in T84 cells by reducing ZO-1 levels and disrupting apical actin, Am. J. Physiol. 276 (1999) G1279–G1288.
[46] R.O. Stuart, A. Sun, M. Panichas, S.C. Hebert, B.M. Brenner, S.K. Nigam, Critical role for intracellular calcium in tight junction biogenesis, J. Cell. Physiol. 159 (1994) 423–433.
[47] T.N. Meyer, C. Schwesinger, J. Ye, B.M. Denker, S.K. Nigam, Reassembly of the tight junction after oxidative stress depends on tyrosine kinase activity, J. Biol. Chem. 276 (2001) 22048–22055.